



ELSEVIER

Journal of Nuclear Materials 283–287 (2000) 789–793

Journal of
nuclear
materials

www.elsevier.nl/locate/jnucmat

Comparison of a microstructure evolution model with experiments on irradiated vanadium

S. Sharafat ^{*}, N.M. Ghoniem

Mechanical and Aerospace Engineering Department, University of California Los Angeles–UCLA, Los Angeles, CA 90095-1600, USA

Abstract

A kinetic rate theory model, which includes the formation of cascade-induced clusters (CIIC), is presented. Comparison of the model to ion irradiation data on vanadium reveals the effects of helium generation and cascade-induced interstitial and vacancy clusters on microstructure evolution. The model is based on a simplification of hierarchical rate equations for the clustering of helium bubbles, immobile vacancy clusters, glissile interstitial clusters, sessile dislocation loops, as well as precipitates and grain boundaries. The model shows that the transport of helium to dislocations, bubbles and grain boundaries is strongly transient because of coupling between the nucleation and growth modes of bubble evolution. Helium agglomeration in vacancy clusters is shown to reduce the excess vacancy flux to grow matrix and precipitate-affixed bubbles. The direct formation of vacancy and interstitial clusters in cascades reduces the growth rate of bubbles, and leads to enhanced nucleation of matrix bubbles. In addition to the dislocation and production bias mechanisms, a new mechanism of ‘helium nucleation bias’ is shown to exist under high helium generation rates. © 2000 Elsevier Science B.V. All rights reserved.

1. Introduction and background

Interaction of high-energy neutrons with fusion reactor materials will result in simultaneous production of displacement damage and helium atoms. Subsequent reactions between helium and defect clusters largely determine most physical and mechanical properties of irradiated materials [1–8]. Vanadium and its alloys are now considered as candidate structural materials in fusion reactors, because of their low neutron activation and high-temperature capabilities. Development of a mechanistic understanding for the influence of helium on microstructure evolution of irradiated vanadium can help in tailoring its microstructure by thermomechanical processes for maximum resistance to radiation damage.

One of the main themes of current interest is the origin of the asymmetry in the flow of vacancies and interstitials to various microstructures. This asymmetry in vacancy/interstitial flow to microstructural features determines the rate of its evolution. In particular, the

growth of voids in irradiated materials was explained in terms of an ‘absorption bias (AB)’ of dislocations towards interstitials, thus leaving excess vacancies to flow into already nucleated voids. Recently, however, another form of asymmetry has been proposed, in which the fraction of free vacancies produced in collision cascades is higher than that of free interstitials [9]. This type of ‘production bias (PB)’ can also lead to cavity growth in irradiated materials, and when combined with AB, can explain qualitative differences in the swelling behavior of bcc and fcc metals [10]. These arguments, however, are based on the notion that cavities have already nucleated in the material, and that their growth phase dominates subsequent evolution.

In the presence of helium production, especially the high levels anticipated under fusion neutron conditions, this scenario might be incomplete. Continuous production of helium in the matrix can result in very long nucleation transients of bubbles. Under these conditions, separation of distinct nucleation and growth phases may not be so clear. During the process of bubble nucleation, helium is trapped in free vacancies to form substitutional sites, from which further agglomeration is possible. If helium production rates are large, the fraction of occupied vacancies, which are tied up with helium-vacancy

^{*} Corresponding author. Tel.: +1-310 825 8917 fax: +1-310 206 4830.

E-mail address: sharafat@ucla.edu (S. Sharafat).

complexes, can be quite substantial. Thus, the balance between free vacancy and interstitial fluxes arriving at those bubbles to allow their growth can be greatly disturbed by helium trapping. This physical scenario can result in an additional complication to the ‘bias’ idea, in which continuous nucleation of helium bubbles can lead to another type of symmetry breaking for free point defects. We will label this effect as the ‘nucleation bias (NB).’

We wish to address the influence of helium on the evolution of irradiated microstructure, with a particular application to the case of irradiated vanadium. We first summarize some of the salient experimental observations on irradiated vanadium microstructure evolution and outline a simplified phenomenological rate theory model in Section 2. Results of the kinetic model are compared to experiments in Section 3. Conclusions and future refinements of the present model are given in Section 4.

2. Simplified kinetic model

The effects of helium generation on the evolution of bubbles in vanadium has been simulated using dynamic helium charging experiments [11] and helium co-implantation during ion irradiation experiments [12,13]. Formation of cavities in the absence of helium has also been extensively studied [14–17]. Irradiation experiments with helium indicate the presence of at least two helium trapping sites for the formation of He-vacancy (HeV) clusters: (1) interstitially dissolved impurities (C, O, N), and (2) fine-size precipitates (e.g., Ti_3Si_3) [2,18,19]. Helium-vacancy clusters that form on precipitates are thermally stable and can grow to create a uniform distribution of helium bubbles. Bubble coalescence at grain-boundaries is therefore not observed in alloyed vanadium. In unalloyed vanadium, HeV clusters, which form on impurities, are thermally unstable above 550 K [2]. This can result in the formation of bubbles with larger sizes compared with those in alloyed vanadium. Depending on the alloy and irradiation temperature, cavity number densities range between 10^{18} and $10^{20} m^{-3}$ with average diameters between 10 and 100 nm for neutron and ion irradiated vanadium. In the presence of helium, either implanted or generated, the formation of HeV clusters on precipitates in alloys or on impurities in unalloyed vanadium is believed to be responsible for the uniform distribution of matrix bubbles [2,18,19].

We introduce here an extension of our rate theory models of helium-vacancy clustering [3,7,8,19], to allow a clear examination of the effects of CIICs and helium on microstructure evolution in vanadium. The model is formulated in the spirit of the ‘mean-field’ approximation, to allow for relatively simple calculations of spatially average microstructure. We also simplify the

problem by ignoring the evolution and spread of microstructure size distribution functions. The model consists of 18 kinetic rate equations, which explicitly account for direct nucleation of both vacancy and interstitial clusters in collision cascades, one-dimensional migration of small interstitial clusters, homogeneous nucleation and growth of bubbles and dislocation loops, as well as the effects of precipitates and grain boundaries on the microstructure. Here we only show the kinetic rate equations for the single vacancies (v), self-interstitials (i), interstitial gas atoms (g), and the substitutional gas-atoms (gv), the complete set of equations are published elsewhere [20].

Following the notation of Ref. [19], the kinetic rate equations for vacancy (v), self-interstitial (i), interstitial helium (g), and substitutional helium (gv), are modified, and respectively given by

$$\begin{aligned} \frac{dC_v}{dt} = & (1 - \varepsilon_v)fG + (\beta e_1 + \delta)C_{gv} \\ & - \{\alpha(C_i + \sqrt{2}C_{2i} + \sqrt{\langle x_{CIIC} \rangle}C_{CIIC}) + \beta C_g \\ & + \gamma(C_s^v + C_{gv} + 2C_{2gv} + 2C_{2g} + 3C^*)\}C_v, \end{aligned} \quad (1)$$

$$\begin{aligned} \frac{dC_i}{dt} = & (1 - \varepsilon_i)fG - \alpha C_i(C_v + C_{gv} + 2C_{2gv} + 3C^* + C_s^i) \\ & - 2\alpha C_i(C_i + \sqrt{2}C_{2i} + \sqrt{\langle x_{CIIC} \rangle}C_{CIIC}), \end{aligned} \quad (2)$$

$$\begin{aligned} \frac{dC_g}{dt} = & G_h + (\beta e_1 + \delta + \alpha C_i)C_{gv} + (\beta e_2 + 2\delta)C_{2gv} \\ & + 3(\delta + \alpha C_i)C^* + 4\delta C_{2g} + 4\alpha C_i C_{2gv} + m\delta C_b \\ & + \delta M_{gb} - \beta C_g\{\varepsilon C_b + C_v + 4C_g + C_{gv} + 2C_{2gv} \\ & + 2C_{2g} + C_{GB} + \varepsilon_{ppt}C_{ppt}\}, \end{aligned} \quad (3)$$

$$\begin{aligned} \frac{dC_{gv}}{dt} = & \beta C_g C_v + (\beta e_2 + 2\delta)C_{2gv} \\ & - C_{gv}\{\beta e_1 + \beta C_g + \delta + \alpha C_i\}. \end{aligned} \quad (4)$$

In these balance equations of the four atomic mobile species, G is the displacement damage rate, G_h the helium production rate, f the fraction of surviving point defects, ε_i the fraction of cascade-induced clustered mobile interstitials, ε_v the fraction of cascade-induced clustered sessile vacancies, and $\langle x_{CIIC} \rangle$ is the average number of interstitial atoms per CIIC. The current model does not include the direct interaction between interstitial helium and cascade-induced clusters. The following notations are used to represent the concentration of species: C_v – vacancy, C_i – single interstitial, C_{2i} – di-interstitials, C_g – interstitial helium, C_{gv} – substitutional helium, C_{2gv} – single vacancy di-hellum cluster, C_{2g} – di-helium interstitial, C_{ppt} – precipitates, C^* – matrix bubble nucleus, m – number of helium atoms per matrix bubble, M_{gb} – number of helium atoms per grain-boundary bubble. The equivalent concentra-

tion of sinks for vacancies, interstitials, and grain boundaries are C_v^s , C_i^s , and C_{GB} , respectively (see Ref. [19] for details).

The attempt migration frequencies of self-interstitials, interstitial helium, and vacancies are α , β and γ , respectively, and are of the form

$$\alpha, \beta, \gamma = 48 \exp(-E_{i,v,He}^m/kT)$$

with $E_{i,v,He}^m$ being the corresponding migration energies. A fourth one, δ , is the helium re-resolution frequency ($\delta = b \times G$), which is proportional to the resolution parameter, b , times the displacement damage rate, G . Thermal emission from helium-vacancy clusters is denoted by e_1 and e_2 and given by $e_{1,2} = \exp(-E_{gv,2g}^B/kT)$, where $E_{gv,2g}^B$ are the binding energies for helium atom to a single vacancy and to a di-helium interstitial cluster, respectively. The term ε and ε_{ppt} are diffusion-controlled combinatorial factors for matrix and precipitate bubbles, respectively: $\varepsilon_{(ppt)} = (4\pi/48)(R_{(ppt)}/a)$. The effective bubble-precipitate pair radius is estimated to be $R_{(ppt)} = (r_p^2 + R_{pb}^2)^{1/2}$, where r_p is the radius of the precipitate and R_{pb} that of a bubble attached to a precipitate.

Additional rate equations are written for small vacancy-helium clusters, containing up to three gas atoms. These equations are then used to calculate the nucleation rate of average size matrix bubbles, and hence their density. Cavities in the matrix, attached to precipitates, and on grain boundaries are treated in an average sense, in which standard growth rate equations are included. To treat the direct formation of sessile and glissile defect clusters in cascades, we include the following additional equations:

$$\begin{aligned} \langle x_{CIVC} \rangle \frac{dN_{CIVC}}{dt} = & \varepsilon_v f G - \rho_{CIVC} (D_i Z_i C_i + \langle x_{CIIC} \rangle \\ & \times D_{CIIC} Z_{CIIC} C_{CIIC} - D_v (C_v - C_{CIVC}^o)), \end{aligned} \quad (5)$$

$$\begin{aligned} \langle x_{CIIC} \rangle \frac{dC_{CIIC}}{dt} = & \varepsilon_i f G - \langle x_{CIIC} \rangle \\ & \times C_{CIIC} D_{CIIC} k_{CIIC}^2, \end{aligned} \quad (6)$$

$$k_{CIIC} = \frac{\pi(\rho + \rho_{CIVC} + \rho_{LOOPS})d_{abs}}{4} + \sigma_b N_b, \quad (7)$$

where x_{CIVC} is the average number of vacancies per CIVC, N_{CIVC} the number density of CIVCs having a radius of r_{CIVC}^o and k_{CIIC} the distributed sink strength for glissile CIICs [20]; d_{abs} the trapping length for mobile species (~ 4 nm); σ_b the absorption cross section of bubbles ($\sigma_b = \pi R_b^2$) and N_b the bubble number density; ρ the dislocation density, ρ_{CIVC} the vacancy loop density, and ρ_{LOOPS} that of the interstitial loops. To estimate ρ_{LOOPS} the number density of interstitial loop nucleus ($N_{i-loops}$) is determined by assuming the loop nucleus concentration to be the sum of the di-interstitials (C_{2i}) plus the concentration of glissile clusters (C_{CIIC}). The

diffusion coefficients for vacancies, interstitials, and CIICs are denoted by D_v , D_i , D_{CIIC} , respectively, and are based on the corresponding migration energies and jump frequencies. The thermal equilibrium concentration of CIVC (C_{CIVC}^o) is based on the thermal detrapping energy of a vacancy from an n -vacancy cluster (E_{nv}^B) and is given by $C_v^e \times \exp(-E_{nv}^B/kT)$ and $C_v^e = \exp(-E_v^F/kT)$ with E_v^F being the vacancy formation energy.

The material parameters for vanadium are published elsewhere [20]. The fraction of cascade-induced interstitial and vacancy clusters, ε_i and ε_v , was taken to be those reported by Phythian et al. [21] for iron, and the irradiation parameters are based on experimental conditions published in references [2,4–6,11–19]. The parameters for the computer simulation were chosen to resemble the experimental conditions published in references [12,13] for irradiated vanadium. Iwai et al. [12,13] reported a precipitate concentration of $\sim 10^{19} \text{ m}^{-3}$, an average grain size of $\sim 30 \mu\text{m}$, and a dislocation density of $\sim 10^{11} \text{ m}^{-2}$. In these experiments, ion-implantation (Ni^+) was used to produce a displacement damage rate of 10^{-3} s^{-1} at temperatures between 700 and 900 K. Helium was co-implanted at a rate of about 5 appm/dpa. Iwai et al. [12,13] reported bubble densities of $\sim 10^{20} \text{ m}^{-3}$ with an average diameter of ~ 70 nm following ion irradiation exposure of 31 dpa at 880 K.

3. Results of computer simulations

Fig. 1 shows the results of the kinetic model without CIIC formation ($\varepsilon_i = \varepsilon_v = 0$) at 880 K, under ion irradiation conditions. During the early stages of irradiation, highly mobile SIAs are soon lost to distributed microstructure sinks, while the relatively slow vacancies are annihilated by SIAs and by the formation of substitutional helium (HeV). Trapping of helium and/or acquiring more vacancies stabilize HeV clusters and forms bubble nuclei. The transient behavior of bubbles thus follows closely that of HeV, which follows that of the single vacancies. HeV clusters grow by absorption of a net flux of single vacancies, and after only $\sim 10^{-4}$ dpa, the vacancy, HeV, and bubble concentration reach equilibrium values of $\sim 10^{22}$, $\sim 10^{20}$ and $\sim 10^{18} \text{ m}^{-3}$, respectively. The evolution of vacancy clusters, interstitial loops, and the dislocation network is simultaneously included in the model, and is presented in [20]. After an irradiation dose of 30 dpa, the current model results in a bubble number density, which is a factor of ~ 100 lower than the experimentally observed density. An average bubble diameter of 160 nm is also reached, which is twice as large as the experimental value of ~ 70 nm [12,13].

Fig. 2 shows the effects of including CIIC formation on the transient evolution of the microstructure. The

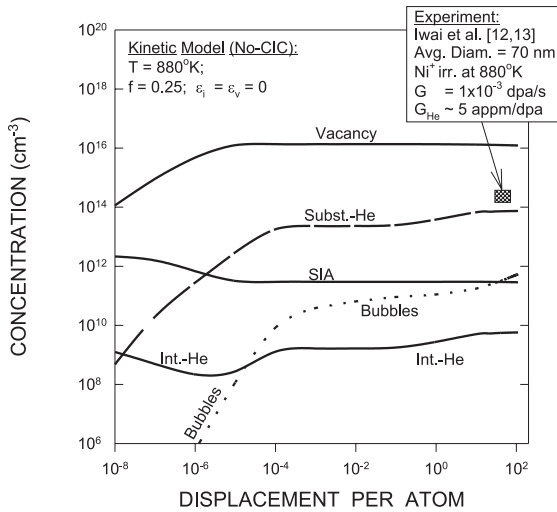


Fig. 1. Microstructure evolution based on kinetic rate theory without cascade-induced vacancy and interstitial cluster formation (Model parameters: $N_{\text{ppt}} = 10^{19} \text{ m}^{-3}$, $R_{\text{ppt}} = 30 \text{ nm}$, grain-size = $3 \mu\text{m}$, $T = 880 \text{ K}$, $G = 1 \times 10^{-3} \text{ dpa/s}$, $G_{\text{He}} = 5 \text{ appm/dpa}$, $f = 0.25$, $\varepsilon_i = \varepsilon_v = 0$).

formation of CIICs results in a significant reduction of free vacancies and SIA's from the very beginning of irradiation. A comparison between Figs. 1 and 2 shows that at $\sim 10^{-5}$ dpa the free vacancy concentration is about $2 \times 10^{18} \text{ m}^{-3}$ while without the production of CIICs it had achieved a high steady state value of

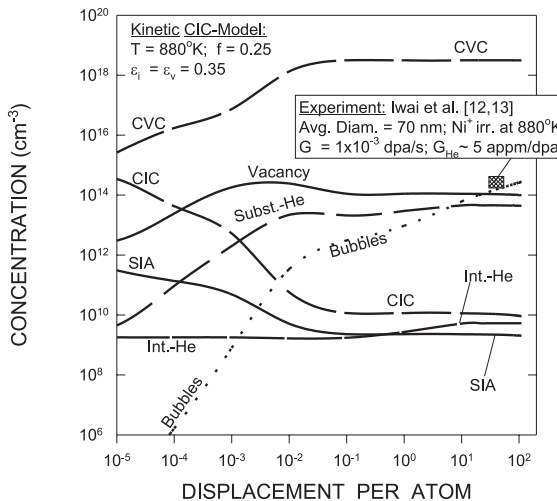


Fig. 2. Microstructure evolution based on kinetic rate theory including cascade-induced vacancy and interstitial cluster formation (Model parameters: $N_{\text{ppt}} = 10^{19} \text{ m}^{-3}$, $R_{\text{ppt}} = 30 \text{ nm}$, grain-size = $3 \mu\text{m}$, dislocation density = 1013 m^{-2} , $T = 880 \text{ K}$, $G = 1 \times 10^{-3} \text{ dpa/s}$, $G_{\text{He}} = 5 \text{ appm/dpa}$, $f = 0.25$, $\varepsilon_i = \varepsilon_v = 0.35$).

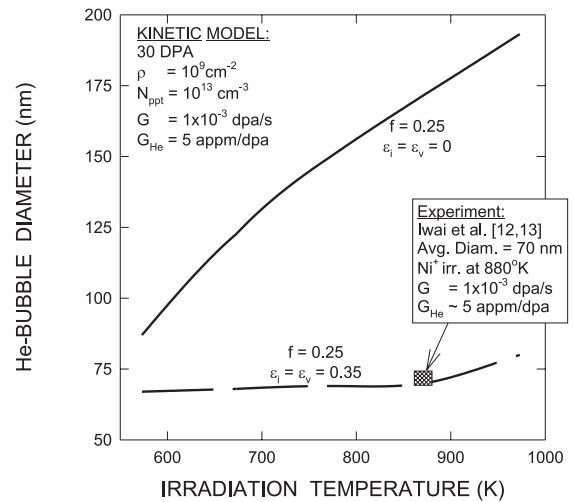


Fig. 3. Average size of helium-filled bubbles for ion-irradiated vanadium as a function of irradiation temperature (Model parameters: $N_{\text{ppt}} = 10^{19} \text{ m}^{-3}$, $R_{\text{ppt}} = 30 \text{ nm}$, grain-size = $3 \mu\text{m}$, dislocation density = 1013 m^{-2} , $T = 880 \text{ K}$, $G = 1 \times 10^{-3} \text{ dpa/s}$, $G_{\text{He}} = 5 \text{ appm/dpa}$, $f = 0.25$, $\varepsilon_i = \varepsilon_v = 0$ and 0.35 without CIIC and with CIIC formation, respectively).

10^{22} m^{-3} . Formation of CIVC and CIIC clusters clearly reduces the concentration of free mobile point defects. Because of the mobility of small interstitial clusters and the reduced number of vacancy clusters, the net flux of vacancies to nucleated cavities is reduced. Thus, this

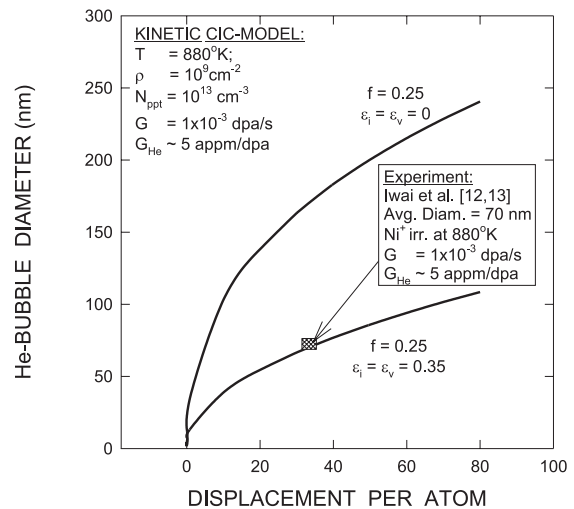


Fig. 4. Average size of helium-filled bubbles in ion-irradiated vanadium as a function of displacement damage (Model parameters: $N_{\text{ppt}} = 10^{19} \text{ m}^{-3}$, $R_{\text{ppt}} = 30 \text{ nm}$, grain-size = $3 \mu\text{m}$, dislocation density = 1013 m^{-2} , $T = 880 \text{ K}$, $G = 1 \times 10^{-3} \text{ dpa/s}$, $G_{\text{He}} = 5 \text{ appm/dpa}$, $f = 0.25$, $\varepsilon_i = \varepsilon_v = 0$ and 0.35 without CIIC and with CIIC formation, respectively).

production bias (PB) leads to a slower growth rate of nucleated bubbles, as compared to the case when CIIC's are not included.

The effect of CIICs on the growth of the bubble size is shown in Figs. 3 and 4. Bubbles grow to physically meaningful sizes of about 70 nm at 30 dpa, which is in very good agreement with experimental data. The direct formation of CIICs in cascades inhibits the fast growth mode of nucleated bubbles, which then leads to an enhancement of nucleation rate, hence the term 'nucleation bias (NB)'.

4. Conclusions

The present model for evolution of bubble, dislocation and defect clusters in irradiated vanadium reveals the delicate balance between rate processes, which control the speed of microstructure evolution. It is clear that bubble nucleation in irradiated vanadium under conditions of high helium generation rates evolves on a long time scale. Strong coupling between the nucleation and growth phases of the microstructure is achieved under these conditions. The presence of helium as an additional specie to intrinsic point defects results in a reduction in the concentration of freely migrating vacancies. The growth rate of nucleated bubbles is thus reduced by the form of natural bias dictated by the presence of helium. Comparison with ion irradiation data shows the necessity to include the direct formation of CIICs in rate theory models, and the need to couple both nucleation and growth phenomena.

Acknowledgements

The authors wish to express their gratitude to Dr B. Singh and Dr S. Gobolov for the many valuable discussions, comments, and suggestions made during the course of this work. Research is supported by the US Department of Energy, Office of Fusion Energy, and Grant DE-FG03-98ER54500 with UCLA.

References

- [1] D.J. Reed, *Radiat. Eff.* 31 (1977) 129.
- [2] A.V. Fedrov, A. van Veen, A.I. Ryazanov, *J. Nucl. Mater.* 233–237 (1996) 385.
- [3] N.M. Ghoniem, S. Sharafat, J.M. Williams, L.K. Mansur, *J. Nucl. Mater.* 117 (1983) 96.
- [4] S.J. Zinkle, H. Matsui, D.L. Samith, A.F. Rowcliffe, E. van Osch, K. Abe, V.A. Kazakov, *J. Nucl. Mater.* 258–263 (1998) 205.
- [5] P.M. Rice, S.J. Zinkle, *J. Nucl. Mater.* 258–263 (1998) 1414.
- [6] J. Gazda, M. Meshii, H.M. Chung, *J. Nucl. Mater.* 258–263 (1998) 1437.
- [7] N.M. Ghoniem, S. Sharafat, L.K. Mansur, in: Jin-Ichi Takamura (Ed.), *Point Defects and Defect Interactions in Metals*, University of Tokyo, 1982, p. 865.
- [8] S. Sharafat, N.M. Ghoniem, *J. Nucl. Mater.* 122 (1–3) (1984) 531.
- [9] C.H. Woo, B.N. Singh, *Phys. Stat. Sol. B* 159 (1990) 609.
- [10] B.N. Singh, *Radiat. Eff. Def. Solids* 148 (1999) 383.
- [11] H.M. Chung, B.A. Loomis, D.L. Smith, *J. Nucl. Mater.* 233–237 (1996) 466.
- [12] T. Iwai, N. Seimura, F.A. Garner, *J. Nucl. Mater.* 239 (1996) 157.
- [13] T. Iwai, N. Seimura, F.A. Garner, *J. Nucl. Mater.* 258–263 (1998) 1512.
- [14] W.J. Weber, G.L. Kulcinski, R.G. Lott, P. Wilkes, H.V. Smith, in: *Proceedings of the International Conference on Radiation Effects and Tritium Technology for Fusion Reactors*, 1–3 October 1975, Oak Ridge National Lab, Gatlinburg, TN, CONF-750989, vol. 1, 1975 pp. 130–149.
- [15] K. Fukumoto, A. Kimura, H. Matsui, *J. Nucl. Mater.* 258–263 (1998) 1431.
- [16] T. Chuto, M. Satou, K. Abe, *J. Nucl. Mater.* 258–263 (1998) 1502.
- [17] A. van Veen, A.V. Fedrov, A.I. Ryazanov, *J. Nucl. Mater.* 258–263 (1998) 1400.
- [18] A.V. Fedrov, A. van Veen, A.I. Ryazanov, *J. Nucl. Mater.* 258–263 (1998) 1396.
- [19] N. Ghoniem, J.N. Alhajji, *J. Nucl. Mater.* 136 (1985) 192.
- [20] S. Sharafat, N.M. Ghoniem, A simplified rate theory model for microstructure evolution with application to irradiated vanadium, to be published in *J. Nucl. Mater.*
- [21] W.J. Phythian, R.E. Stoller, A.J.E. Foreman, A.F. Calder, D.J. Bacon, *J. Nucl. Mater.* 223 (1995) 245.